UNIVERSITY OF MINNESOTA

This is to certify that I have examined this copy of a master's thesis by

Rebecca Sue Nestingen

and have found that it is complete and satisfactory in all respects,
and that any and all revisions required by the final
examining committee have been made.

Name of Faculty Co-Adviser	Name of Faculty Co-Adviser

Signature of Faculty Co-Adviser	Signature of Faculty Co-Adviser

Date

GRADUATE SCHOOL

The Comparison of Infiltration Devices and Modification of the Philip-Dunne
Permeameter for the Assessment of Rain Gardens

A THESIS
SUBMITTED TO THE FACULTY OF THE GRADUATE SCHOOL
OF THE UNIVERSITY OF MINNESOTA
BY

Rebecca Sue Nestingen

IN PARTIAL FULFILLMENT OF THE REQUIREMENTS
FOR THE DEGREE OF
MASTER OF SCIENCE

John S. Gulliver, Raymond M. Hozalski, and John L. Nieber

November 2007

Acknowledgements

Dedication

I'd like to dedicate this thesis to my husband, Jens, and my parents, Jim and Sue, for their support and encouragement in pursuing a higher level degree. And also to Brooke Asleson, who has not only played the role of a fellow researcher, but has become a good friend. She was always there when I needed someone who would listen to and understand my frustrations and accomplishments along the way.

Abstract

A Modified Philip-Dunne (MPD) falling head infiltrometer was developed for measuring surface infiltration rates in stormwater best management practices (BMPs). The MPD consists of a hollow cylinder that is simply inserted into the soil surface rather than into a borehole like the Philip-Dunne (PD) permeameter. The analysis developed by Philip for the PD permeameter was modified to account for differences in flow geometry for the MPD configuration so that the saturated hydraulic conductivity (K_s) and wetting front suction (C) of the soil could be determined from head versus time data. The accuracy of the modified analysis procedure was verified by comparing the K_s and C values obtained by fitting simulated head versus time data from a finite element solution of the Richards equation for homogenous and isotropic soils with the values used as inputs for the simulations. The error in estimated K_s and C obtained from the Modified Philip-Dunne analysis ranged from -1.8% to -15% and 6.4% to 62%, respectively for parameter values representing soils ranging from silty clays to coarse sands.

The MPD was then compared against the double-ring infiltrometer and the Minidisk® infiltrometer in the laboratory for accuracy and precision using three types of sand. Accuracy was determined by comparing the hydraulic conductivity values obtained using these devices with those obtained by reference falling head tests. The Modified Philip-Dunne infiltrometer was the most accurate across three sand media of different particle size while the double-ring infiltrometer was the most precise. The Modified Philip-Dunne infiltrometer followed the double-ring in precision. The MPD and the corresponding analysis described herein should prove useful for assessing the stormwater infiltration characteristics of infiltration-based BMPs such as rain gardens.

Table of Contents

List of Tables

List of Figures

Role of Author

The research conducted in this thesis was performed by Brooke Asleson, myself, and others research team members cited in the acknowledgements section. Brooke Asleson and I coordinated the research with the guidance of our advisors John Gulliver, Ray Hozalski, and John Nieber. I was the primary contributor to the research in this thesis. The work contained in this thesis represents a portion of the work conducted by myself and Brooke Asleson.

1 Project Overview

This thesis contains research work that stems from two stormwater projects: the "Assessment of Stormwater BMPs" funded by the Minnesota Pollution Control Agency (MPCA) and "Assessment of Stormwater Treatment Practices on the Quantity and Quality of Runoff" which was funded by the Metropolitan Council Environmental Services (MCES) and the Minnesota Local Road Research Board (LRRB). The overarching goal of the first project was to develop an *Assessment of Stormwater Best Management Practices Manual* to serve as a guidance document for permitted municipal separate storm sewer systems (MS4s). The resulting guidance document entails a four level approach to assessment of stormwater BMPs. These four levels are: (1) visual inspection, (2) capacity testing, (3) synthetic runoff testing, and (4) monitoring. The second project, "Assessment of Stormwater Treatment Practices on the Quantity and Quality of Runoff", aimed to develop and implement testing techniques for underground proprietary devices and rain gardens/bioretention facilities.

Several University of Minnesota Departments and Centers took part in this large scope project including Bioproducts and Biosystems Engineering, Civil Engineering, University of Minnesota Extension, St. Anthony Falls Hydraulic Laboratory, and the Water Resources Center. In addition to the University of Minnesota departments listed the following external organizations also contributed to the project: City of Bloomington, City of Plymouth, Dakota County Soil and Water Conservation District, Ramsey Washington Metro Watershed District, Three Rivers District, Washington County Conservation District, and the Wisconsin Department of Natural Resources.

The particular portion of the stormwater projects that this thesis is associated with is the assessment of rain gardens. The rain garden assessment in itself consisted of a team effort and is made up of the following components: development of an assessment approach (B. Asleson thesis), evaluation and comparison of several infiltration devices (this thesis), modification to the selected permeameter (this thesis), implementation of the assessment approach to several rain gardens (B. Asleson thesis), and the evaluation of the assessment results (B. Asleson thesis). The need for an evaluation and comparison of infiltration devices and the modifications to the Philip-Dunne permeameter arose from the development of a rain garden assessment approach and the subsequent application of the approach. For the evaluation of the assessments performed at several rain gardens the work in this thesis supports and improves the accuracy of the assessment results.

2 Modifications to the Philip-Dunne Permeameter

2.1 Introduction

Infiltration basins, infiltration trenches, rain gardens (bioretention practices), and related stormwater best management practices (BMPs) reduce runoff volume primarily via infiltration into the subsurface (Winogradoff, 2002; Dietz and Clausen, 2005). If the infiltration rate is too slow, stormwater may overtop or otherwise bypass the BMP (Winogradoff, 2002). Furthermore, slow infiltration rates can lead to prolonged periods of inundation, mosquito problems, and plant failure (Winogradoff, 2002). Thus, infiltration rate is an important indicator of the functionality of these BMPs.

Devices used to measure infiltration rate of surface soils include: the tension infiltrometer, the Minidisk infiltrometer (from Decagon Devices), the Guelph permeameter, and the double ring infiltrometer. Each of these devices, however, suffers from one or more of the following limitations: relatively high volume of water required (double-ring, tension), experimental duration (double-ring, Guelph, tension), difficulty of setup and operation (tension, Guelph), cost (tension, Guelph), and inaccuracy (Minidisk) (Johnson, 2006; Asleson, 2007).

The original Philip-Dunne (PD) permeameter is a relatively simple, effective, and inexpensive falling head device that is used to determine the infiltration properties of shallow subsurface soil. A test is performed with the device inserted into a borehole to a depth of about 15 cm. Because the Philip-Dunne permeameter is inserted into a borehole, the infiltration capacity of the surface soil is not measured. This is problematic for use in infiltration BMPs because the surface infiltration rate could be limiting due to

accumulation of fine particles (i.e. silts and clays) transported into the BMP by the stormwater. Thus, a new device was developed and named the Modified Philip-Dunne (MPD) infiltrometer that has the same advantages as the Philip-Dunne permeameter but is inserted into the surface soil to a depth of about 5 cm. This modification changes the geometry of the infiltrating flow so it is not possible to use the borehole analysis of Philip (1993) to derive the hydraulic properties of the soil. The purpose of this paper is to introduce the MPD infiltrometer and the theory needed to solve for the hydraulic properties of the soil from measurements made with the infiltrometer.

2.2 Methods

2.2.1 Device Construction

The MPD infiltrometer, shown in Figure 2.1, consists of an open ended cylinder constructed out of 2 mm-thick, 10 cm inner-diameter aluminum pipe. The bottom edge of the cylinder is beveled from the outside to ease the process of inserting the device 5 cm into the soil surface. At a height of 5 cm from the bottom, a hole is drilled for the addition of an elbow joint to connect a clear plastic piezometer tube to the outside of the cylinder. Alongside the piezometer tube a metric measuring tape is adhered to the cylinder with the zero marking beginning at the elbow joint (5 cm from the bottom of the cylinder). Inside the cylinder a fine mesh screen is adhered to cover the hole and prevent fine soil particles from clogging the elbow joint and piezometer tube.
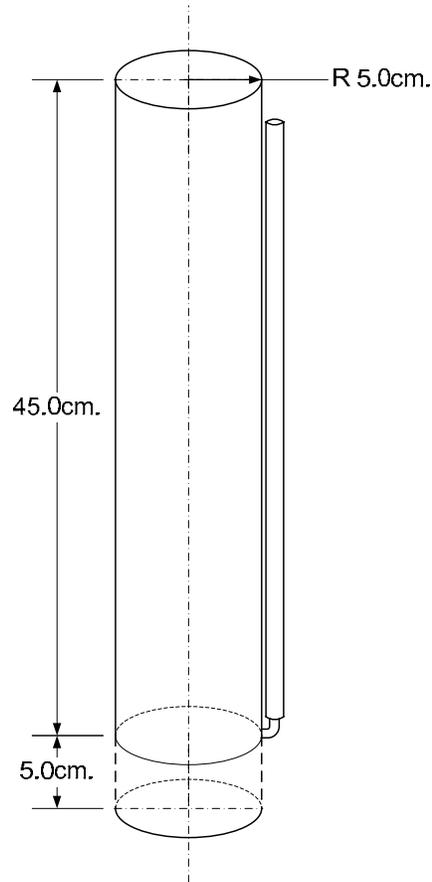
Figure 2.1: Diagram of a Modified Philip-Dunne infiltrometer.

A mounting bracket (not shown), connected to the top of the cylinder with a metal rod, is used to support an ultrasonic sensor. The ultrasonic sensor measures water level automatically at a frequency of 1 Hz and the water level values are then averaged over 10 seconds. The ultrasonic sensor allows for more precise and frequent measurements (as opposed to manually recording the height within the piezometer tube) for purposes of calibrating the device.

2.2.2 Device Operation

The MPD infiltrometer is inserted into the soil surface to a depth of 5 cm. Initial soil moisture measurements are then made from locations (five in our case) around the

outside edge of the device at the soil surface. These measurements are made gravimetrically (Klute, 1986; ASTM, 2000, 2005) or with a calibrated moisture probe (e.g., ThetaProbe®). Soil moisture before and after the infiltration measurement is required for computing the hydraulic properties of the soil. The infiltration test is performed by filling the device to a predetermined initial height, H_0, and then recording the head in the device over time. At least three measurements (initial, midpoint, and final) of head versus time are required to characterize the falling head curve (Munoz-Carpena, et al., 2002). Nevertheless, significantly more data can be obtained with the ultrasonic sensor or by making more frequent measurements with the piezometer and a stopwatch. Immediately upon completion of the test the device is removed and five final moisture measurements are made from the soil that was within device in the same manner as the initial moisture measurements.

2.3 Analysis

2.3.1 Effect of Flow Geometry on Infiltration Rate

The geometry of flow around the infiltrometer, both for the original Philip-Dunne borehole configuration and the modified configuration used herein has a significant effect on the infiltration rate into the soil. We have not attempted to measure this effect experimentally, but here we will show the effect using a numerical model.

The governing equation used for this demonstration is Richards' equation, the common equation used for modeling flow in unsaturated soils. The three-dimensional axi-symmetric form of this equation is:

$$\frac{\partial \theta}{\partial t} = \frac{1}{r}\frac{\partial}{\partial r}\left(Kr\frac{\partial h}{\partial r}\right) + \frac{\partial}{\partial z}\left(K\frac{\partial h}{\partial z}\right) + \frac{\partial K}{\partial z} \qquad (2.1)$$

6

where, θ = volumetric water content, K = unsaturated hydraulic conductivity, assumed to be isotropic, h = water pressure head, r, z = radial and vertical coordinates, and t = time. The K-θ relationship is modeled by van Genuchten (1980) as

$$K(S_e) = K_s S_e^{0.5} \left[1 - (1 - S_e^{1/m})^m\right]^2 \qquad \text{(2.2a)}$$

and

$$\theta = \theta_r + \frac{\theta_s - \theta_r}{\left[1 + (\alpha h)^n\right]^m} \qquad \text{(2.2b)}$$

where

$S_e = \dfrac{\theta - \theta_r}{\theta_s - \theta_r}$, $m = 1 - \dfrac{1}{n}$, θ_s = saturated water content, θ_r = residual water content, and

α, n = van Genuchten parameters from soil-water retention curve. The numerical solution to Equation 2.1 is based on a finite element formulation and implemented through the earth science module of a commercial software package (COMSOL, 2007).

The flow domain of interest for the Philip-Dunne is represented by the axisymmetric region illustrated in Figure 2.2. For this domain all boundaries are treated as impermeable except for the bottom boundary, which is treated as a unit gradient boundary, and the soil surface inside the tube which has a time varying pressure specified by the mass balance of the water initially poured into the tube, decreasing due to infiltration as time progresses.

The initial conditions for an infiltration event are uniform water pressure approximately equal to the water pressure at field capacity for the soil. Water is poured into the infiltrometer tube to a specified depth (in our case this was 43 cm), and the

infiltration event continues until the initial volume of water has completely infiltrated into the soil. For the simulations to follow, the van Genuchten parameters (van Genuchten, 1980) used were those representing a medium sand ($\alpha = 4m^{-1}$, $n = 4$, $\theta_s = 0.375$, $\theta_r = 0.05$, $K_s = 1.65x10^{-4} m/\sec$).

Simulation results for the PD case with a 15 cm deep borehole are shown in Figure 2.2. Similar simulations were run for the MPD, illustrated in Figure 2.3. The flow configuration for the PD (Figure 2.2) is similar to that shown in Figure 2.3 except that the soil is not augured out. The differences between the two simulations of Figure 2.2 and Figure 2.3 are that the MPD was inserted into the soil to a depth of 5 cm.
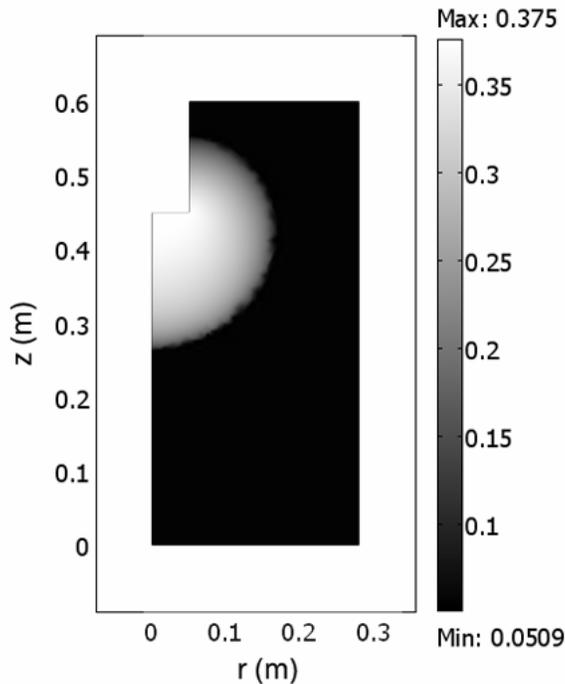
Figure 2.2: Simulated axi-symetric distribution of the volumetric moisture content for a 15 cm borehole (PD) at the conclusion of the run (145 seconds).

8
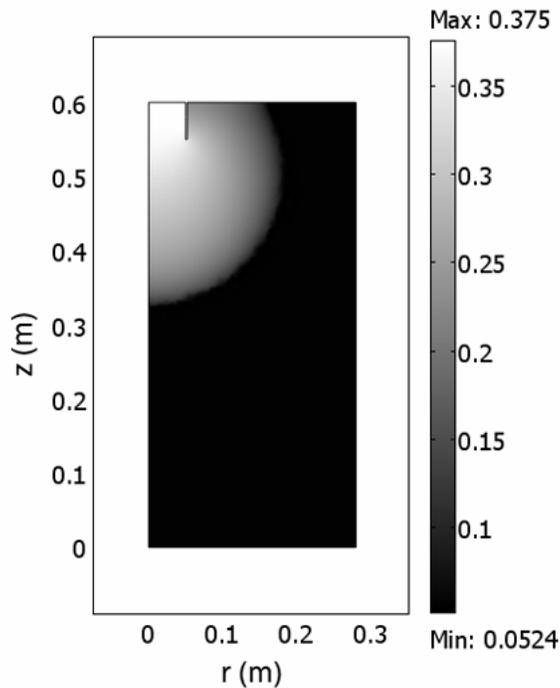
Figure 2.3: Simulated axi-symetric distribution of the volumetric moisture content for a 5 cm penetration depth (MPD) at the conclusion of the run (470 seconds).

There are significant differences in the flow patterns for the two cases. First, the water in the MPD passes one-dimensionally through the 5 cm long encased soil core before three-dimensional flow into the soil beneath and around the infiltrometer commences. In addition, the wetting front from the infiltrated water reaches the soil surface in the MPD (i.e. a capped sphere geometry), resulting in a smaller wetted volume available for the MPD than for the borehole case. These flow constraints for the MPD resulted in a longer time for the infiltrometer tube to empty.
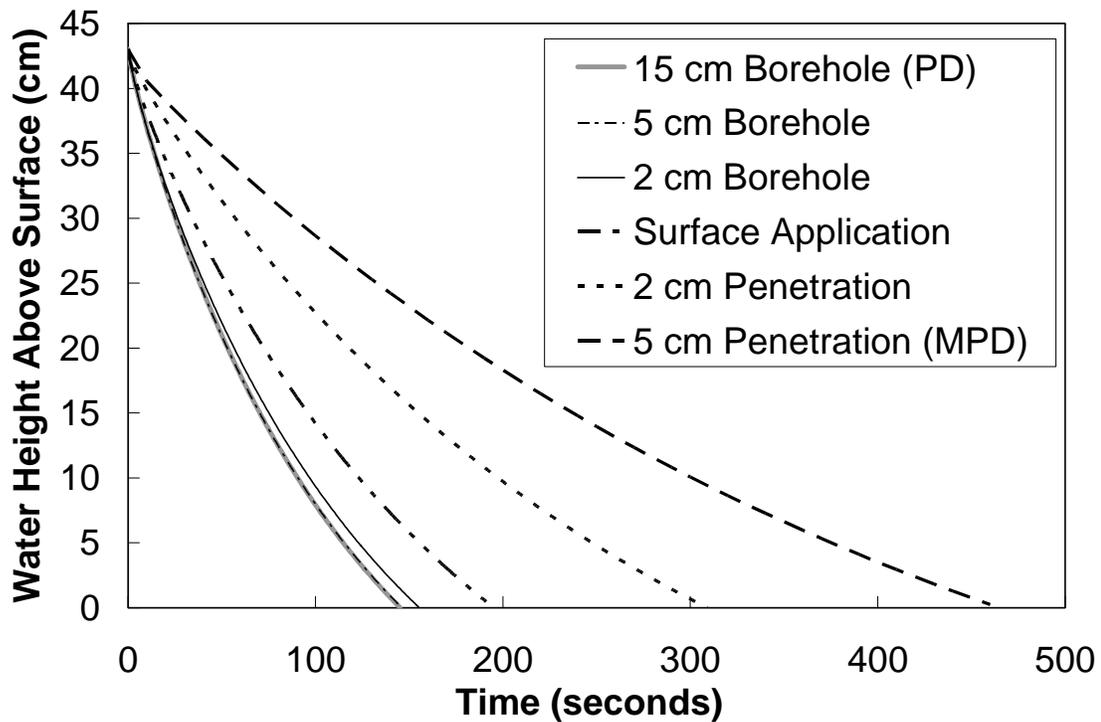
Figure 2.4: Simulation results at several penetration and borehole depths.

The results from several simulation runs for different borehole depths for the conventional PD and penetration depths for the MPD are presented in Figure 2.4. The water level versus time behavior for the PD case is insensitive to the borehole depth for depths greater than 5 cm. The simulated PD drain time increases noticeably, however, for more shallow borehole depths of 2 cm and 0 cm (i.e. surface application). The main reason for the increase in drain time is the transition from a spherical wetting front to a capped sphere for the shallower borehole depths.

The effect of changing penetration depth of the MPD configuration is apparent from the plots while the PD permeameter drain time is insensitive to changes in borehole depth. The confining of the flow through the soil encased inside of the infiltrometer tube

10

slows the rate of drop of the water level inside the tube. The time required to empty the infiltrometer for a 5 cm tube penetration is more than twice that required for the case of surface application, and about 30% more than for the case of 2 cm penetration. This results from the pressure loss that occurs in transmitting the water through the encased soil volume. It is thus prudent to know the penetration depth of the MPD infiltrometer quite accurately, in contrast to the PD permeameter where the rate of water drop is relatively insensitive to the depth of the borehole.

2.3.2 MPD Infiltrometer Model

Philip (1993) developed a mathematical model for use in analyzing permeameter data for the PD geometry. That model, however, is not applicable for the MPD flow geometry. As a result, it is necessary to derive a modification to the Philip borehole permeameter model. Philip's analysis assumes an isotropic homogeneous media, a Green-Ampt sharp wetting front and an ideal spherical geometry for the wetting front by subtracting the gravitational component of the flow. The source of the infiltrating flow is assumed to be a sphere with a surface area equivalent to the bottom circular surface area of the cylinder. The flow velocity is separated into two components that reflect the gradients in the gravitational and the pressure-capillarity forces (Philip, 1993). A similar approach is taken for the analysis of the Modified Philip-Dunne infiltrometer. Due to the application of the device at the surface rather than in a borehole, however, the no-flow boundary at the soil surface outside of the cylinder is taken into account by representing the wetted soil as a capped sphere. In addition to modifying the geometry of flow, the pressure loss across the soil encased within the inserted portion of the device needs to be incorporated. The necessary modifications are described in the following.

11

The subsequent notation is used in the Modified Philip-Dunne infiltrometer equations in correspondence to the illustration presented in Figure 2.5: H_0, the initial height of water; $H(t)$, the height of water at time t; L_{max}, the depth of insertion into the soil; r_0, the equivalent source radius; r_1, the radius of the cylinder; r, any radius within the wetted front; $R(t)$, the radius to the sharp wetted front at time t.
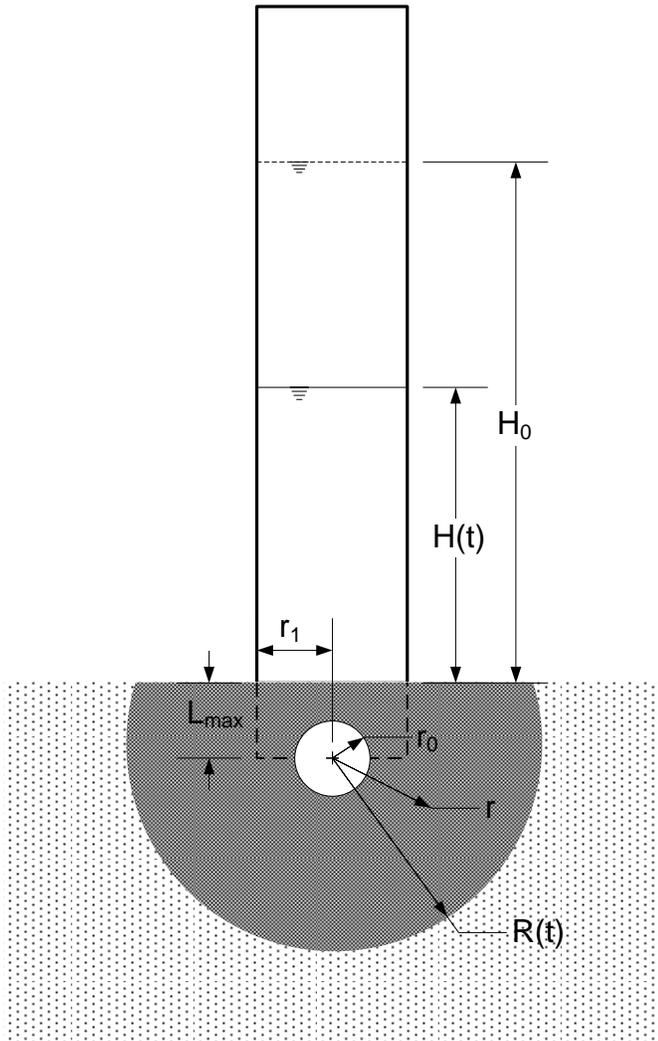
Figure 2.5: Important parameters of the MPD infiltrometer.

The analysis considers herein only the portion of the falling head curve from $R(t) > \sqrt{r_1^2 + L_{max}^2}$ to when the cylinder is completely empty. Prior to the wetted

12

front reaching this minimal radius, the head versus time data are neglected from the analysis because the geometry of the wetting front changes, requiring a different series of equations. It is during this initial period of time that the infiltration front is contained inside of the encased cylinder of soil. The time to reach this value of $R(t)$ is relatively small, so the additional equations were of little help in determining hydraulic conductivity. After Philip (1993), a new equation for cumulative infiltration, $i(t)$ is obtained by assuming a capped sphere geometry where the sphere has a height of $R(t) + L_{max}$ and the soil has an initial and final moisture content of θ_0 and θ_1, respectively.

$$i(t) = \frac{\pi}{3}(\theta_1 - \theta_0)\left(2[R(t)]^3 + 3[R(t)]^2 L_{max} - L_{max}^3 - 4r_0^3\right)$$ (2.3)

Note that in the analysis of Philip a full sphere and not a capped sphere was assumed. A mass balance on the water in the infiltrometer and the water that has infiltrated into the surface is used to compute $R(t)$ as a function of $H(t)$ for use in the MPD analysis:

$$[H_0 - H(t)]r_1^2 = \frac{(\theta_1 - \theta_2)}{3}\left[2[R(t)]^3 + 3[R(t)]^2 L_{max} - L_{max}^3 - 4r_0^3\right].$$ (2.4)

By following the same analysis procedure as Philip (1993), which involves integrating (2.4 and then separating the velocity into pressure-capillary and gravitational components, the pressure-capillary flow velocity component, $v_c(r)$, for $r_0 < r < R(t)$ becomes

$$v_c(r) = \left[(\theta_1 - \theta_0)\left([R(t)]^2 + [R(t)]L_{max}\right)\frac{dR}{dt} - 2r_0^2 \overline{K}\right]\frac{1}{r^2 + rL_{max}}$$ (2.5)

where $\overline{K}$ is the mean hydraulic conductivity in the wetted soil, assumed to be equal to the saturated hydraulic conductivity, K_s. Integrating Equation 2.5 with respect to r and

13

applying Darcy's law, the pressure-capillarity potential drop, $\Delta P(t)$, from the spherical source to the wetted front becomes

$$\Delta P(t) = \frac{\pi^2}{8}\left\{(\theta_1 - \theta_0)\frac{[R(t)]^2 + [R(t)]L_{max}}{\overline{K}}\frac{dR}{dt} - 2r_0^2\right\} \times \frac{\ln\left[\dfrac{R(t)[r_0 + L_{max}]}{r_0[R(t) + L_{max}]}\right]}{L_{max}} \qquad (2.6)$$

where $\pi^2/8$ (Philip, 1993) is applied to account for the actual flow geometry at the base of the permeameter and the assumed geometry of a spherical source. To calculate the pressure loss due to the soil encase within the device, Darcy's law is used to obtain the following equation to approximate pressure at the surface of the spherical source, P_0:

$$P_0 = H(t) + L_{max} - \frac{L_{max}}{\overline{K}}\frac{dH}{dt}. \qquad (2.7)$$

Therefore, the total pressure-capillarity potential drop from the spherical source to the wetted front is given by

$$\Delta P(t) = C - H(t) - L_{max} + \frac{L_{max}}{\overline{K}}\frac{dH}{dt} \qquad (2.8)$$

where C is the wetting front suction for the unsaturated soil. The wetting front suction is defined as

$$C = \int_{h=h(\theta_0)}^{h=0} K(h)dh. \qquad (2.9)$$

Equation 2.4 is used to solve for $R(t)$. Equations 2.6 and 2.8 are then used to solve for $\Delta P(t)$ with assigned values of $\overline{K}$ and C. The solution is achieved by minimizing the sum of the square of the differences between the values of $\Delta P(t)$ calculated from Equations

2.6 and 2.8. Note that the experimental measurements of the water depth in the permeameter tube are directly embedded in these calculations.

2.3.3 Solution Procedure

A computational technique was developed to obtain values of $\overline{K}$ and C based on the equations presented above. For the following computational procedure, Microsoft Excel® was used with the Solver Add-In and Visual Basic Application to find solutions to Equations 2.4, 2.6, and 2.8; automate the computational process; and obtain values of $\overline{K}$ and C. The general procedure for finding values of $\overline{K}$ and C is:

1. Input all measured variables, including the radius of the device, the depth of insertion into the soil, initial moisture, final moisture, initial height, and the head versus time curve.

2. For each measurement of head use the relationship in Equation 2.4 to find the corresponding distance of the sharp wetting front (note: solver and a macro were used to automate this step).

3. Estimate the change in head with respect to time and the change in wetting front distance with respect to time by using the backward difference for all values of $R(t)$ equal to or greater than the distance $\sqrt{r_1^2 + L_{max}^2}$.

4. Make initial guesses for the values of $\overline{K}$ and C.

5. Solve Equations 2.6 and 2.8 for $\Delta P(t)$ at each incremental value of t.

6. Minimize the absolute difference between the two solutions found in step 5 by adjusting the values of $\overline{K}$ and C. Solver was used to find the best fitting values that produced a minimum sum of the squared differences in ΔP.

15

2.3.4 MPD Model Verification

To check the accuracy of the equations for the Modified Philip-Dunne infiltrometer falling head data were simulated using the finite element program (COMSOL, 2007) and the solution procedure was applied to estimate the specified hydraulic properties of the synthetic soils. The soil properties of the synthetic soils were defined in terms of van Genuchten (1980) parameters. A range of parameters were used to represent a range of soil textures.

The procedure for each test was as follows: a set of values for $\theta_0, \theta_1, \alpha, n, K_s, H_0$ was defined as inputs to the finite element model. The time dependent drop in water level inside the infiltrometer tube was derived from this infiltration simulation. Using the head versus time curve from the simulation, the defined change in moisture, and geometry of the infiltrometer, values of $\overline{K}$ and C were obtained using the analysis procedure described above. These parameter values were then compared to the values specified for the finite element solution. The value of C corresponding to the simulations was derived using Equation 2.9 with the assigned van Genuchten parameters.

2.4 Results and Discussion

For the following model simulations the values for H_0, θ_0, and θ_1 were held constant at 43 cm, 0.055 and 0.375, respectively, while values for the van Genuchten parameters, α and K_s were varied using linear scaling theory (Vogel et al., 1991). According to this theory, a reduction in α by a factor X has a corresponding reduction in K_s by a factor X^2. The van Genuchten parameter n was kept constant at 4.0. The initial and final moisture content values were set to give a large change in moisture content in order to simulate the sharp wetting front assumed in the Philip (1993) analysis. Finally,

16

K_s was varied from 2.97 x 10^{-7} m/s to 6.60 x 10^{-4} m/s and wetting front suction was varied from 1.74 m to 0.087 m to represent soil textures ranging from a silty clay to coarse sands (Rawls et al., 1983).

A comparison of the assigned parameters for the synthetic soils with the values derived using the Modified Philip-Dunne infiltrometer analysis procedure for an insertion depth of 5 cm, diameter of 10 cm, and initial water height of 43 cm is shown in Table 2.1.

Table 2.1: Comparision of K_s and C from the Modified Phillip-Dunne model and finite element simulations.

	Saturated Hydraulic Conductivity (m/s)			Wetting Front Suction (m)		
	COMSOL Model	Modified Theory	Error	COMSOL Model	Modified Theory	Error
Case A	2.97 x 10^{-7}	2.67 x 10^{-7}	-10.0%	0.249	0.233	-6.4%
Case B	7.40 x 10^{-7}	6.82 x 10^{-7}	-7.9%	0.249	0.230	-7.7%
Case C	1.65 x 10^{-6}	1.40 x 10^{-6}	-15%	1.740	2.012	15.7%
Case D	3.80 x 10^{-6}	3.51 x 10^{-6}	-7.6%	0.249	0.229	-8.1%
Case E	1.13 x 10^{-5}	1.05 x 10^{-5}	-7.0%	0.249	0.227	-8.7%
Case F	4.13 x 10^{-5}	3.86 x 10^{-5}	-7%	0.340	0.401	18.0%
Case G	9.27 x 10^{-5}	9.11 x 10^{-5}	-1.8%	0.249	0.216	-13.2%
Case H	1.65 x 10^{-4}	1.58 x 10^{-4}	-4%	0.174	0.221	26.8%
Case I	6.60 x 10^{-4}	6.19 x 10^{-4}	-6%	0.087	0.141	62.4%

The modified theory underestimates K_s by 4% (Case H) to 15% (Case C) for the cases examined. The error in determination of the wetting front suction ranged from -13.2% to 62.4%. The greatest absolute error in wetting front suction estimation was for the case of the coarse sand, which had an extremely low wetting front suction value, otherwise the error was less than 27%. Fortunately, the MPD model results were not highly sensitive to wetting front suction and similar discrepancies between the wetting front suction determined by the PD and other infiltrometers were demonstrated by Munoz-Carpena, et al. (2002) and Gómez et al. (2001).

A slight but consistent underestimation of K_s was observed which is believed to be due to the distortion of the actual flow path lines caused by the no-flow boundaries of the device and the soil surface. By plotting K_s from the finite element simulations against the computed K_s from the MPD theory and fitting a linear trendline through the data, a correction factor of 1.064 was obtained. Thus, the corrected K_s (K_s') can be computed as follows

$$K_s{}' = 1.064 K_s.$$ (2.10)

3 Laboratory Comparison of Field Infiltrometers

3.1 *Introduction*

Hydrologists, engineers, and soil scientists measure the infiltration rate and hydraulic conductivity of porous media for a variety of purposes such as designing clay liners for solid waste facilities or determining drainage of pavement base material. Infiltration is also important for stormwater management. Many stormwater best management practices (BMPs) such as rain gardens, infiltration basins, vegetated swales, and porous pavement rely on infiltration as a primary means to reduce the volume of stormwater runoff. Furthermore, such BMPs also remove pollutants from the water via filtration, sorption, and other mechanisms as the water percolates through the soil matrix.

The field methods that exist for measuring hydraulic conductivity of soil vary broadly in applicability and accuracy (ASTM D-5126, 2004). Generally, infiltrometers measure hydraulic conductivity at the soil surface and permeameters measure hydraulic conductivity at various depths in a soil profile. Common devices used in the field include: single and double ring infiltrometers, air-entry permeameters, and borehole permeameters (ASTM D-5126, 2004). The device used is often dependent upon criteria for a specific scenario (i.e. falling head devices may be preferred over constant head devices when measuring materials with low hydraulic conductivities). In this study, field devices were selected for comparison based on the applicability to measure hydraulic conductivity of rain gardens. Because fine particles transported by stormwater may accumulate at the soil surface and limit infiltration, it was desired to select devices that capture the effect of the soil surface. Additional criteria for device selection include

transportability of equipment, volume of water needed, experiment duration, simplicity of operation, cost, and personnel requirements (Johnson, 2006; Asleson, 2007).

Based on these criteria the double-ring infiltrometer, Minidisk infiltrometer (Decagon Devices), and a Modified Philip-Dunne (MPD) infiltrometer were chosen for further evaluation. The double-ring infiltrometer is a well-established field method for measuring infiltration and computing hydraulic conductivity, however, due to simplifying assumptions of one dimensional flow and a unit hydraulic gradient, the accuracy of this device is only fair relative to air-entry and borehole permeameter methods (ASTM D-5216, 2004). The Minidisk infiltrometer is a small tension infiltrometer that draws on a method developed by Zhang (1997) to determine the hydraulic conductivity and sorptivity of a soil. The MPD is a new falling head device developed in our laboratory for determining the hydraulic conductivity of surface soils, thus, converting it from a permeameter (Dunne and Safran, see Philip, 1993) to an infiltrometer.

The accuracy and precision of these devices have not been thoroughly evaluated and compared in a single study. Munoz-Carpena et al. (2001) compared field Philip-Dunne permeameter results with results obtained from a lab permeameter using a core of soil from the same site. The *in situ* saturated hydraulic conductivity determined by the Philip-Dunne permeameter was approximately one third of that determined by the laboratory constant head permeameter. Potential explanations for the difference in hydraulic conductivity are the heterogeneity of the soil in the field and compaction and disturbance to soil structure during core collection, transport, and installation in the laboratory permeameter. No controlled laboratory studies that would minimize these potential differences have been conducted to compare the accuracy and precision of these

devices. Thus, controlled laboratory testing was conducted to compare the accuracy and precision of the double-ring infiltrometer, Minidisk infiltrometer, and newly developed MPD.

3.2 Methods

3.2.1 Experiment Set-up

A sufficient surface area and depth of soil was required to operate the selected infiltrometers. Barrels with a diameter of 56 cm, height of 91 cm, and volume of 208 liters (Greif, Inc.) were chosen as vessels for the calibration media. Each barrel was fitted with a threaded PVC valve along the side near the bottom that allowed the media to drain. A thin coating of sand was attached to the inner walls of the barrels with a spray adhesive to roughen the surface and minimize the potential for preferential flow of water along the walls. A layer of 7.6 cm of pea gravel was placed at the bottom of the barrel and covered with a coarse filter fabric to isolate the gravel from the media above. A homogeneous sand media was added over the filter fabric to a height of 50.8 cm, stopping periodically to tamp down the sand to prevent large voids and non-uniform compaction.

Three media were used for the comparisons: (1) 100% ASTM C-33 sand (barrel 1), (2) 80% (by weight) ASTM C-33 sand with 20% US Silica F110 sand (barrel 2), and (3) 100% US Silica F110 sand (barrel 3). The media were selected to represent a range of relatively high permeability engineered soils used in rain gardens and other infiltration BMPs. The Prince George's County Bioretention Manual recommends using 50%-60% clean ASTM C-33 construction sand with 20%-30% sandy loam/loamy sand and 20%-30% leaf compost material for a soil medium (Windogradoff, 2002). Other manuals

recommend similar mixes, although in application the compost is often omitted. The compost material was omitted from our media in order to achieve homogeneous mixtures that would not change over time due to degradation of organic material. The particle size distributions for each sand mixture were determined by a sieve analysis (ASTM C136) and are given in Figure 3.1. The sand media was mixed in a portable mortar mixer before addition to the barrels.
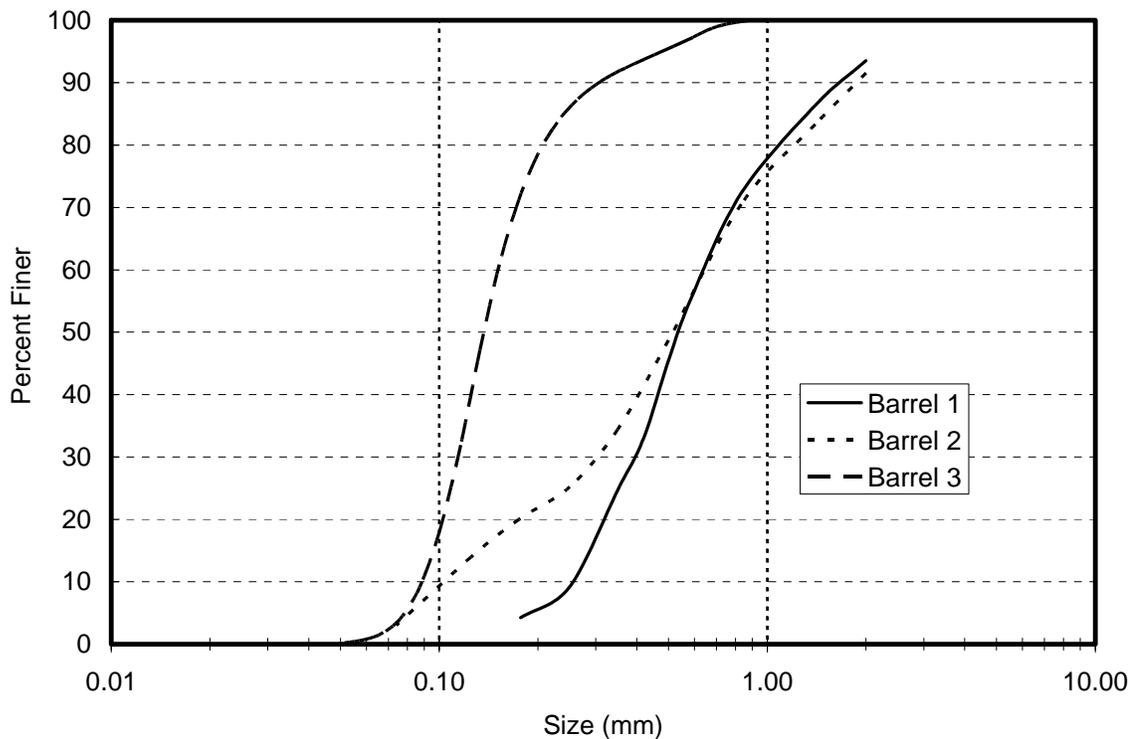
Figure 3.1: Particle size distribution of the three media used for infiltration testing.

3.2.2 Device Operation

3.2.2.1 Double-Ring Infiltrometer

The custom made double-ring infiltrometer used in this research was slightly smaller in diameter than most commonly used double-ring infiltrometers (ring diameter dimensions of 30 cm and 60 cm) to permit insertion into the barrel opening. The dimensions of the outer and inner rings were 20 and 40 cm, respectively, keeping the

22

standard value of two for ratio of the diameters of the outer and inner rings (ASTM D-3385, 2003). The device was situated at the center of the barrel to keep the distance from the edge of the barrel equivalent around the circumference and then uniformly driven into the sand to a depth of 5 cm. Each ring was then filled with water from two different supply carboys. The head in the inner ring was maintained at a constant level through the use of a Mariotte bottle and the head was maintained manually at approximately the same depth in the outer ring. Once a constant head was achieved in both rings the volume within the carboy supplying the inner ring was recorded at regular time intervals and used to determine the infiltration rate of the sand.

3.2.2.2 Minidisk Infiltrometer

The Minidisk Infiltrometer (Figure 3.2) has a base diameter of 4.5 cm and an infiltration volume around 90 mL. Tests were performed at five different locations on the surface of the media to account for any local heterogeneity of the media and to determine a spatially averaged hydraulic conductivity. The suction was set to 6 cm for each test as recommended in the Minidisk Infiltrometer User's Manual (Decagon Devices, 2005) for sandy soils with high infiltration rates. The sintered steel disk was placed directly on the smooth surface of the sand and the volume within the device was recorded at a regular time interval until the water reservoir was empty.

Figure 3.2: Illustration of the Minidisk infiltrometer (Source: Decagon Devices, 2005).

3.2.2.3 Modified Philip-Dunne Infiltrometer

The MPD infiltrometer (Figure 3.3) was developed to measure the hydraulic conductivity of the surface soil material, in contrast to the measurement below the surface in-borehole measurement for the original Philip-Dunne device. The MPD infiltrometer is inserted into the sand to a depth of 5 cm. Initial moisture content of the sand was measured at five locations around the edge of the device and the device was filled with water to a height of 43 cm. Water surface elevation was recorded over time during the test with an ultra-sonic sensor mounted above the device. Head data can also be collected manually using the clear piezometer tube on the side of the device (Figure 3.3) and a stopwatch. Immediately upon the device reaching empty it was removed from the barrel and five final moisture content measurements were made.

R 5.0cm.

45.0cm.

5.0cm.
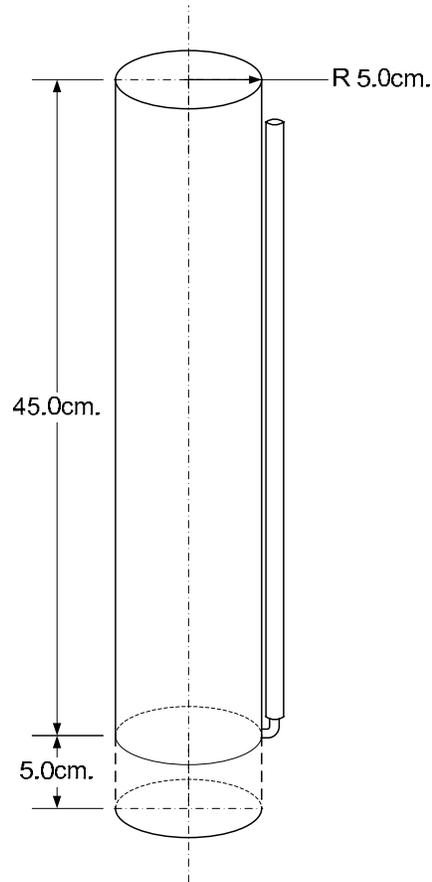
Figure 3.3: Modified Philip-Dunne infiltrometer developed for study.

3.2.3 Soil Moisture Measurements

The change in volumetric soil moisture content is needed to determine the saturated hydraulic conductivity from the MPD infiltrometer test. Two methods were used to determine volumetric soil moisture content: direct measurement from a calibrated soil moisture probe (specifically, a ThetaProbe®) and gravimetric soil moisture measurement. The relationship given in Equation 3.1 was used convert the measured gravimetric moisture content, θ_g to volumetric moisture content, θ_v with a measurement of the bulk density (density of the solids, water and air) of the soil, ρ_b.

$$\theta_v = \theta_g \cdot \rho_b \qquad\qquad \textbf{(3.1)}$$

25

The ThetaProbe® uses time-domain reflectometery to measure the apparent dielectric constant, ε. The device output (V) is linearly related to the square root of the dielectric constant, $\sqrt{\varepsilon}$ which is in turn related to volumetric moisture content. The relationship between the dielectric constant and volumetric moisture content is soil specific following the general relationship

$$\sqrt{\varepsilon} = a_0 + a_1 \cdot \theta_v \qquad\qquad (3.2)$$

in which a_0 and a_1 are the soil specific calibration coefficients (Delta-T Devices, 1999). The values were determined to be 1.6, 1.7, and 1.6 for coefficient a_0 and 9.6, 8.3, and 7.6 for coefficient a_1 of barrels 1, 2, and 3, respectively.

3.2.4 Reference Falling Head Tests

To perform a reference falling head test the barrel was filled at an approximate flow rate of 5 mL/s from a hose connected to a valve at the bottom. This method of filling the barrels from the bottom up at low flow was used to minimize entrapped air in the soil voids. The flow rate during filling was maintained below that required to fluidize of the sand so as not to disturb the bed. When the barrel was nearly full at a water level approximately 20 cm above the sand surface the valve was closed and the hose was disconnected. An ultra-sonic sensor was then mounted to the top of the barrel. The valve at the bottom was opened and the head versus time data were recorded automatically (6 readings per minute).

3.3 Analysis

3.3.1 Double-Ring Infiltrometer

The steady-state infiltration rate in the inner ring was determined according to ASTM D-3385 (2003) standard methodology. Applying Darcy's law and assuming a hydraulic gradient of one, the saturated hydraulic conductivity is equivalent to the steady-state infiltration rate.

3.3.2 Minidisk Infiltrometer

The cumulative infiltration, I, is described by the following function

$$I = C_1 \sqrt{t} + C_2 t \tag{3.3}$$

where t is time and C_1 and C_2 are parameters defining the sorptivity and hydraulic conductivity, respectively (Philip, 1969). The values for C_1 and C_2 were obtained by plotting the measured cumulative infiltration against the square root of time and fitting a second order polynomial equation. C_2 is related to the hydraulic conductivity at the applied tension according to the following relationship (Zhang, 1997):

$$C_2 = A_2 K \tag{3.4}$$

where A_2 is a dimensionless coefficient

$$A_2 = \frac{11.65(n^{0.1} - 1)\exp\left[2.92(n - 1.9)\alpha h_0\right]}{(\alpha r_0)^{0.91}} \quad n \geq 1.9 \tag{3.5}$$

$$A_2 = \frac{11.65(n^{0.1} - 1)\exp\left[7.5(n - 1.9)\alpha h_0\right]}{(\alpha r_0)^{0.91}} \quad n < 1.9 \tag{3.6}$$

and n and α (cm^{-1}) are van Genuchten (1980) moisture retention parameters for the soil, r_0 (cm^{-1}) is the radius of the infiltrometer disk, and h_0 (cm^{-1}) is the tension at the soil surface (Decagon Devices, 2005).

Because the soil in all three barrels is classified as sand by soil texture, grain-size distributions were used rather than texture classification to obtain distinct van Genuchten parameters for each barrel. The van Genuchten parameters, α and n, can be estimated from the grain-size distribution (Jonasson, 1989) as

$$n = -0.0983 + \frac{1}{1.0566L - 0.5487L^2 + 0.1008L^3} \tag{3.7}$$

and

$$\alpha = \frac{(0.75^{-1/(1-1/n)} - 1)^{1/n}}{h_{75}} \; (\text{m-1}) \tag{3.8}$$

where $\qquad L = \log(h_{25}/h_{75})$, $\qquad h_{25}/h_{75} = (d_{75}/d_{25})^{1+\beta}$, $\qquad \beta = 3(\alpha_{AP} - 1)/2$,

$\alpha_{AP} = \exp 0.312 \log(d_{75}/d_{25})$, $\; h_{75} = \dfrac{0.0364}{e^{1/2} d_{75}^{1+\beta}} (720.7W_F)^{\beta/3}$ (m), $e = (\rho_s - \rho_b)/\rho_b$, $W_F =$

0.01, ρ_s = particle density, ρ_b = bulk density, d_{25} = grain diameter for 25% cumulative by weight (mm), and d_{75} = grain diameter for 75% cumulative by weight (mm). The n values were 2.33, 1.72, and 4.19 for barrels 1, 2, and 3, respectively and the α values were 0.155, 0.168, and 0.026 cm^{-1} for barrels 1, 2, and 3, respectively. These van Genuchten parameter values combined with a disk radius of 2.2 cm and a tension of 6 cm resulted in A_2 values of 0.85, 5.99, and 8.60 for use in Equation 3.4 to compute the hydraulic conductivity at a moisture content corresponding to 6 cm of tension.

3.3.3 Modified Philip-Dunne Infiltrometer

The Modified Philip-Dunne infiltrometer theory assumes that the infiltration into the soil can be separated into two flow components: the gravimetrical flow component and capillary-pressure flow component (Philip, 1993). The capillary-pressure flow

28

component when examined independently of gravitational flow causes the assumed sharp wetted front to take on the geometry of a spherical cap with the soil surface being a no-flow boundary. Assuming flow from a spherically equivalent source with a radius equal to half of the cylindrical radius as in Philip (1993) and that the flow is one-dimensional through the 5 cm depth of the insert, Equation 3.9 is obtained for the MPD infiltrometer:

$$C - H(t) - L_{max} + \frac{L_{max}}{\overline{K}}\frac{dH}{dt} = \frac{\pi^2}{8}\left\{(\theta_1 - \theta_0)\frac{[R(t)]^2 + [R(t)]L_{max}}{\overline{K}}\frac{dR}{dt} - 2r_0^2\right\}$$

$$\times\left\{\frac{\ln[R(t)[r_0 + L_{max}]/r_0[R(t) + L_{max}]]}{L_{max}}\right\}$$

(3.9)

where C = wetting front suction (m), H = head of water above the surface (m), t = time (s), L_{max} = depth of device penetration in soil (m), $\overline{K}$ = mean hydraulic conductivity (m/s), θ_0 = initial volumetric moisture (unitless), θ_1 = final volumetric moisture (unitless), R = radius to the sharp wetted front (m), and r_0 = spherical source radius (m).

Due to the initial phase of the test being poorly represented by a capped spherical geometry, Equations 3.9 and 3.10 apply for $R(t) \geq \sqrt{r_1^2 + L_{max}^2}$. The radial distance to the sharp wetting front, $R(t)$ is determined according to the mass balance

$$[H_0 - H(t)]\pi r_1^2 = \frac{(\theta_1 - \theta_0)\pi}{3}\left[2[R(t)]^3 + 3[R(t)]^2 L_{max} - L_{max}^3 - 4r_0^3\right]$$

(3.10)

where H_0 is the initial head of water (m), r_1 is radius of the cylindrical tube (m), and all other parameters are previously defined. The two unknown soil properties $\overline{K}$ and C are determined by minimizing the sum of absolute difference between each side of Equation 9 for two or more time increments. To obtain accurate estimates of $\overline{K}$ and C, the data for most of the drawdown curve (i.e. for $R(t) > \sqrt{r_1^2 + L_{max}^2}$) was used rather than only 3

points as in Munoz-Carpena et al. (2001). This allowed for better estimates of $\dfrac{dH}{dt}$ and

$\dfrac{dR}{dt}$ in Equation 3.9 through the backwards difference technique. Lastly a factor of 1.064

was applied to obtain $\overline{K}' = 1.064\overline{K}$ from numerical model simulations. It was assumed

that $\overline{K}' \approx K_s$, the saturated hydraulic conductivity (Philip, 1993).

3.3.4 Reference Falling Head Test

The analysis for the reference falling head test is similar to the analysis of a

falling head lab permeameter. In the case of a falling head, the flow and hydraulic

gradient are both time dependent. Darcy's law is used to calculate saturated hydraulic

conductivity, K_s from the following equation

$$K_s = \frac{L}{\Delta t} \ln\left[\frac{h_i + L}{h_{i+1} + L} \right] \qquad (3.11)$$

where L is the length of the soil column, and h_i and h_{i+1} are ponded head depths at the

beginning and end of the time interval Δt. The barrels were conditioned by performing

approximately seven reference falling head tests before beginning the actual experiments.

The conditioning phase was performed to allow the media in the barrels to settle and

compact and to determine the filling flow rate that would not fluidize the media.

The mean hydraulic conductivity determined by each of the devices tested were

compared to the mean hydraulic conductivity of the reference falling head tests. The

error of each device relative to that of the reference falling head test is defined as

$$Relative\ Error = \frac{\overline{x}_i - \overline{x}_r}{\overline{x}_r} \times 100\% \qquad (3.12)$$

$$Absolute\ Error = \frac{\left|\bar{x}_i - \bar{x}_r\right|}{\bar{x}_r} \times 100\%$$ **(3.13)**

where x_i is the hydraulic conductivity determined from the device and x_r is the hydraulic conductivity determined from the reference falling head test.

3.3.5 Treatment of Outliers

Outliers in each dataset were identified (and removed from further consideration) using the median and median absolute difference (MAD) method developed by Rousseeuw (1990) with a critical value of 2.5. The outliers were removed to obtain a dataset free of erroneous measurements caused by experimental error such as equipment malfunctions and operator error.

3.4 Results

3.4.1 Summary of Datasets

The arithmetic mean of the hydraulic conductivity values (excluding outliers) for the three sands measured with each device are presented in Figures 3.4 to 3.6 with corresponding descriptive statistics in Tables 3.1 to 3.3. Only 5.2% of the test results (10 out of 192) were identified as outliers. Outliers were randomly distributed among the different devices and barrels.
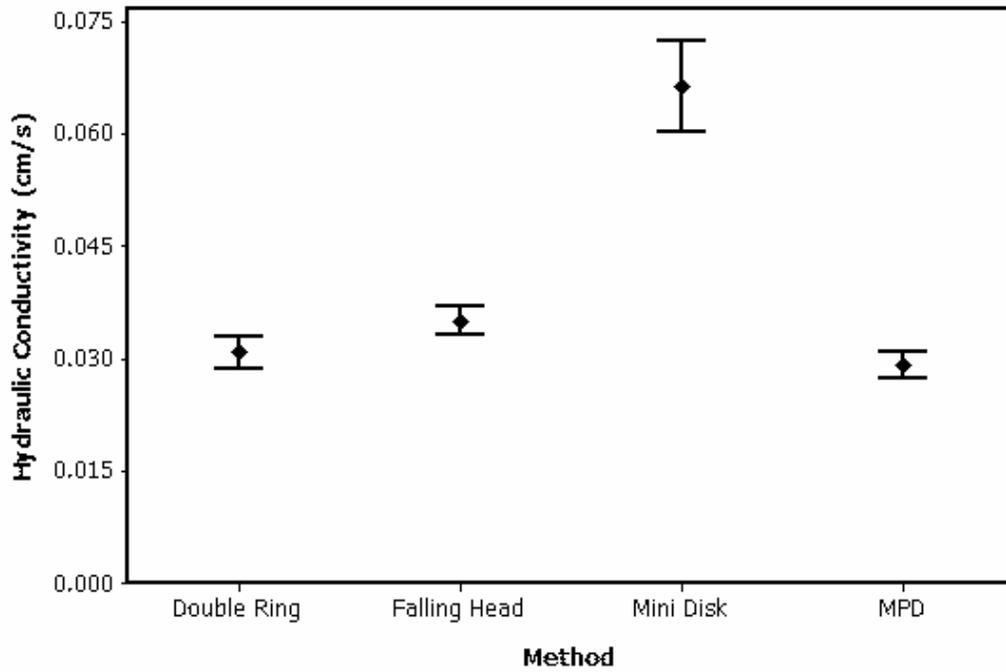
Figure 3.4: Comparison of mean hydraulic conductivity values determined using the three devices and reference falling head tests for barrel 1. Error bars represent 95% confidence intervals.
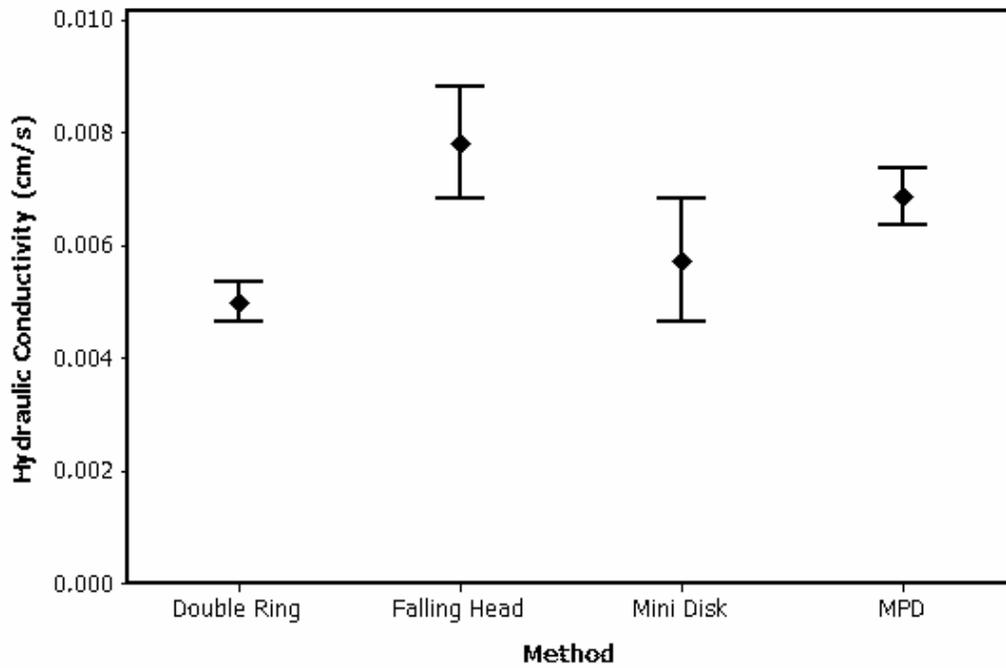
Figure 3.5: Comparison of mean hydraulic conductivity values determined using the three devices and reference falling head tests for barrel 2. Error bars represent 95% confidence intervals.
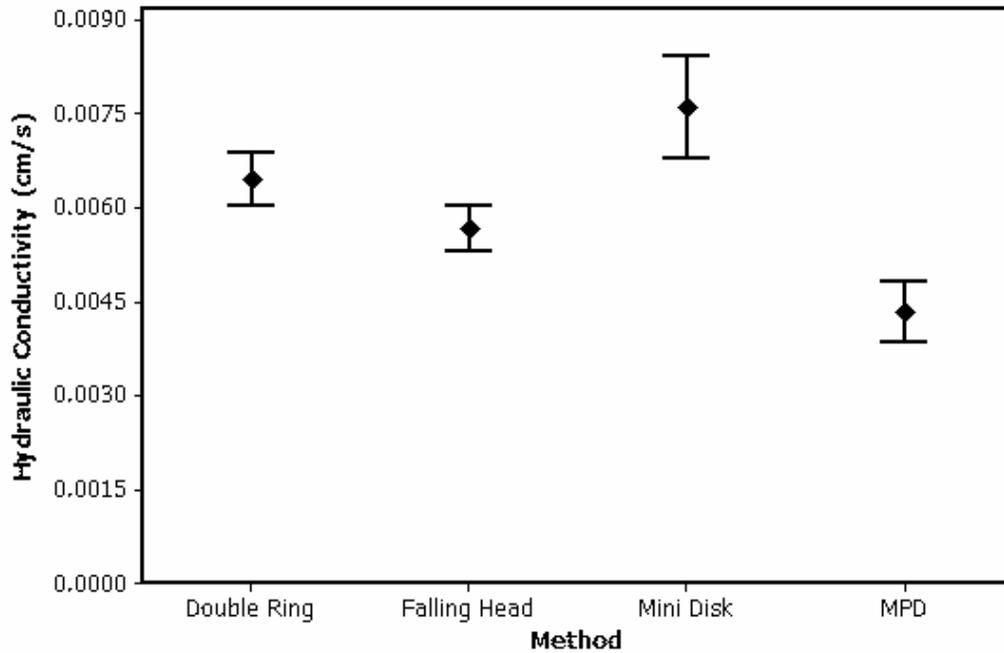
Figure 3.6: Comparison of mean hydraulic conductivity values determined using the three devices and reference falling head tests for barrel 3. Error bars represent 95% confidence intervals.

Table 3.1: Descriptive statistics for hydraulic conductivity of barrel 1. *N* represents the sample size.

	MPD	Mini Disk	Falling Head	Double Ring
Min. (cm/s)	0.0249	0.0516	0.0261	0.0268
Max. (cm/s)	0.0335	0.0817	0.0451	0.0339
Mean (cm/s)	0.0291	0.0664	0.0350	0.0308
Median (cm/s)	0.0291	0.0682	0.0350	0.0312
Std. Dev. (cm/s)	0.0025	0.0084	0.0046	0.0023
CV	8.5%	12.7%	13.0%	7.6%
Skewness	0.18	-0.04	-0.04	-0.72
Kurtosis	-0.17	0.53	-0.23	0.45
N	11	10	25	7

Table 3.2: Descriptive statistics for hydraulic conductivity of barrel 2. *N* represents the sample size.

	MPD	Mini Disk	Falling Head	Double Ring
Min. (cm/s)	0.0050	0.0029	0.0042	0.0043
Max. (cm/s)	0.0092	0.0097	0.0117	0.0059
Mean (cm/s)	0.0069	0.0057	0.0078	0.0050
Median (cm/s)	0.0068	0.0055	0.0077	0.0049
Std. Dev. (cm/s)	0.0010	0.0021	0.0021	0.0005
CV	14.5%	35.9%	26.9%	9.9%
Skewness	0.46	0.68	0.47	0.74
Kurtosis	0.60	-0.29	-0.50	0.04
N	17	16	20	10

Table 3.3: Descriptive statistics for hydraulic conductivity of barrel 3. *N* **represents the sample size.**

	MPD	Mini Disk	Falling Head	Double Ring
Min. (cm/s)	0.0031	0.0047	0.0047	0.0057
Max. (cm/s)	0.0063	0.0105	0.0075	0.0077
Mean (cm/s)	0.0043	0.0076	0.0057	0.0065
Median (cm/s)	0.0042	0.0078	0.0056	0.0063
Std. Dev. (cm/s)	0.0010	0.0015	0.0008	0.0006
CV	23.1%	19.6%	14.2%	9.9%
Skewness	0.37	-0.16	1.16	0.79
Kurtosis	-1.27	0.20	0.78	-0.40
N	19	15	21	11

For barrel 1 (Figure 3.4 and Table 3.1), the mean hydraulic conductivity value determined by the Minidisk is approximately twice that of the other devices. For barrel 2 (Figure 3.4 and Table 3.2) and barrel 3 (Figure 3.6 and Table 3.3), results for all of the methods are more similar. The coefficients of variation (CV) for all the tests are relatively low and range from 7.6% to 35.9%. Munoz-Carpena et al. (2002) reported CV values of 38.9% to 101.2% when comparing permeameters in the field. Lower CV values would be expected for a controlled laboratory comparison because the sand media without compost material is homogenous in comparison to field soils. The skewness and kurtosis values indicate that the datasets may be described as normally distributed. This could also be a consequence of the relatively homogenous sands used in the testing. Comparatively, it is typical for field measured hydraulic conductivity to be represented by a lognormal distribution (Asleson, 2007).

3.4.2 Comparison of Methods

To compare the measurement methods to one another through analysis of variances, the probability distributions and variances of the datasets need to be approximately the same (Toothaker, 1994). The empirical distribution functions of the

datasets were compared to a normal probability distribution function using the Anderson-Darling test statistic, A^2 that describes the goodness-of-fit. The Anderson-Darling test is more powerful than Pearson's chi-square goodness-of-fit test for small sample sizes. A sample size (N) adjustment factor given in Equation 3.14 was used to obtain A^{2*} (Stephens, 1986).

$$A^{2*} = A^2 \left(1 + \frac{0.75}{N} + \frac{2.25}{N}\right)$$ (3.14)

The values of A^{2*} for fit of the datasets to a normal distribution are shown in Table 3.4. A critical value of A^{2*} of 0.752 corresponding to a significance level of 5% was selected. A value of A^{2*} greater than the critical value results in a rejection of the assumed normal distribution (Stephens, 1986).

Table 3.4: Adjusted Anderson-Darling test statistic, A^{2*}.

	MPD	Mini Disk	Falling Head	Double Ring
Barrel 1	0.141	0.296	0.269	0.288
Barrel 2	0.189	0.391	0.595	0.307
Barrel 3	0.837	0.170	1.020	0.500

From Table 3.4, the assumed normal distribution is accepted at a significance level of 5% for all of the datasets for barrels 1 and 2. For barrel 3, the Mini Disk and double ring datasets are accepted at a significance level of 5% while the the normal distribution is rejected for the MPD and reference falling head test datasets. A test for homogeneity of the variances was conducted and the P-values for Levene's test of equal variances are 0.017, 0.005, and 0.022 for barrels 1, 2, and 3, respectively (Brown and Forsythe, 1974). Each of the P-values is less than 0.05 and thus the null hypothesis that variances are equal is rejected. Because the assumptions of normality and equal

variances are violated a robust multiple comparison procedure is required, hence, the selection of the Games and Howell (GH) procedure (Toothaker, 1993).

The results of the GH procedure for comparison of the means for each of the barrels are shown in Table 3.5. The means from both the Minidisk and double ring were significantly different at a 5% level from the reference falling head test means in all three barrels. In comparison the means from the MPD were statistically different from the reference falling head tests for barrels 1 and 3 but not for barrel 2. For barrel 1, a significant difference in the mean hydraulic conductivity at the 5% level is shown between all method combinations except the MPD and double ring. Conversely, barrel 2 shows significantly different means between the MPD and double ring as well as the Minidisk-reference falling head test and double ring-reference falling head test combinations. The results of the barrel 3 comparison demonstrated a significant difference in means for all method combinations except the Minidisk and double ring.

Table 3.5: Mean difference of hydraulic conductivity (cm/s)by measurement method (* represents significant difference in means at the 5% level). Value in parentheses is the P-value.

(I) Measurement Method	(J) Measurement Method	Barrel 1 Mean Difference (I-J)	Barrel 2 Mean Difference (I-J)	Barrel 3 Mean Difference (I-J)
MPD	Mini Disk	-0.0373(0.00)*	0.0011(0.22)	-0.0033(0.00)*
	Falling Head	-0.0059(0.00)*	-0.0010(0.29)	-0.0013(0.00)*
	Double Ring	-0.0017(0.47)	0.0019(0.00)*	-0.0021(0.00)*
Mini Disk	MPD	0.0373(0.00)*	-0.0011(0.22)	0.0033(0.00)*
	Falling Head	0.0314(0.00)*	-0.0021(0.03)*	0.0019(0.00)*
	Double Ring	0.0355(0.00)*	0.0008(0.50)	0.0011(0.07)
Falling Head	MPD	0.0059(0.00)*	0.0010(0.29)	0.0013(0.00)*
	Mini Disk	-0.0314(0.00)*	0.0021(0.03)*	-0.0019(0.00)*
	Double Ring	0.0041(0.02)*	0.0029(0.00)*	-0.0008(0.03)*
Double Ring	MPD	0.0017(0.47)	-0.0019(0.00)*	0.0021(0.00)*
	Mini Disk	-0.0355(0.00)*	-0.0008(0.50)	-0.0011(0.07)
	Falling Head	-0.0041(0.02)*	-0.0029(0.00)*	0.0008(0.03)*

Comparing the MPD, Minidisk, and double ring hydraulic conductivity values to the reference falling head test values, the MPD consistently underestimated the K_s compared to the reference value. The relative error for each device compared to reference falling head tests is displayed in Figure 3.7.
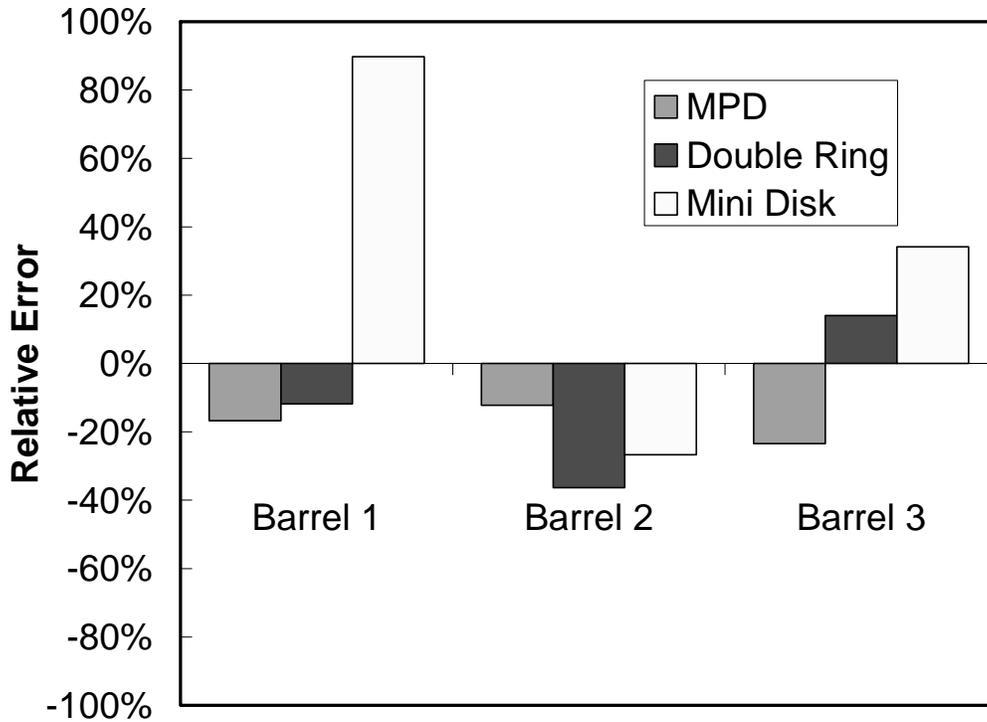

Figure 3.7: Comparison of relative error in hydraulic conductivity obtained by the three devices for the three media used in the testing

4 Conclusions and Future Work

The analysis of Philip for the Philip-Dunne borehole permeameter was modified for use with a device developed for infiltration measurements at the soil surface termed the MPD infiltrometer. The accuracy of the modified analysis procedure was verified by comparing the saturated hydraulic conductivity (K_s) and wetting front suction (C) values obtained by fitting simulated falling head versus time data from a finite element solution of the Richards equation with the values used as inputs for the simulations. The error in estimated K_s and C obtained from the Modified Philip-Dunne analysis ranged from -1.8% to -15% and 6.4% to 62%, respectively for parameter values representing soils ranging from silty clays to coarse sands.

From laboratory testing, the double ring was the most precise of the three devices as it had the lowest CV for all three of the media used in the testing. The MPD device was typically the second most precise of the three devices. According to the statistical analysis, none of the methods was consistently accurate (in comparison to the reference falling head test) but the MPD and double ring were the most accurate of the 3 methods for the sand media used in the testing. The average absolute error for the double ring was slightly higher than that of the MPD although the average relative error across all three barrels for the double ring was less than that for the MPD. The error of the Minidisk was the highest error of all three devices and the hydraulic conductivity of the sand in barrel 1 was overestimated by a large amount (90%).

An underestimate of the saturated hydraulic conductivity via the Minidisk method is to be expected. This is due to the reality that the moisture content of the sand may not reach saturation at a 6 cm tension. Nevertheless, the minidisk only underestimated the

saturated hydraulic conductivity in barrel 2. Therefore, a more likely explanation for the error observed from the sensitivity of hydraulic conductivity to estimating the correct van Genuchten parameters for the sand.

Nonetheless, all of the devices produced reasonably accurate results when considering the orders of magnitude by which hydraulic conductivity values can vary in the field. Some of the theoretical assumptions for the analysis of hydraulic conductivity, such as the media being homogeneous and isotropic that were acceptable in the laboratory setting typically would be violated in a field setting. Thus, the error for each device would be expected to increase in the field. Future work is needed to evaluate the effect of violating the assumption of homogenous-isotropoic media. The inclusion of organic material and/or macropores would better represent soil present in the field.

Overall, estimates of hydraulic conductivity obtained using the MPD infiltrometer were similar in accuracy and precision to one of the most commonly used field devices, the double ring infiltrometer. The MPD shows great potential for applications in the field due to the comparatively short duration of a test, ease of use, lower volume of water required, and lower cost of device construction (Asleson, 2007). The MPD and the corresponding analysis described herein should prove useful for assessing the stormwater infiltration characteristics of infiltration-based BMPs such as rain gardens.

5 References

A.S.T.M. D2216-05, 2005. Standard Test Method for Laboratory Determination of Water (Moisture) Content of Soil and Rock by Mass. ASTM International, Ed.

A.S.T.M. D3385-03, 2003. Standard Test Method of Infiltration Rate of Soils in Field Using Double-Ring Infiltrometer. ASTM International, Ed.

A.S.T.M. D5126-90, 2004. Standard Guide for Comparison of Field Methods for Determining Hydraulic Conductivity in Vadose Zone. ASTM International, Ed.

Asleson, B.C. 2007. The development and application of a four-level rain garden assessment, M.S. Thesis, University of Minnesota, Minneapolis.

Brown, B. Morton and Alan B. Forsyte. 1974. Robust Tests for the Equality of Variances. Journal of the American Statistical Association. 69: 364-367.

COMSOL AB. 2006. COMSOL Multiphysics Users Guide. Version 3.3 Documentation.

Decagon Devices, Inc. 2005. Mini Disk Infiltrometer User's Manual Version 1.4. Pullman, Washington.

Delta-T Devices Ltd. 1999. ThetaProbe Soil Moisture Sensor User Manual. Cambridge, England.

Dietz, M.E. and J.C. Clausen. 2005. A field evaluation of rain garden flow and pollutant treatment. Water, Air, and Soil Pollution. 167:123-138.

Gómez,J.A., J.V. Giráldez, and E.Fereres. 2001.Analysis of infiltration and runoff in an olive orchard under no-till. Soil Science Society of America Journal. 65:291–299.

Johnson, S.M. 2006. Evaluation of the Philip-Dunne Permeameter in determination of the effectiveness of alternative storm water practices, Plan B, University of Minnesota, St. Paul.

Jonasson, S. A. 1989. Estimation of the van Genuchten parameters from grain-size distribution. In Indirect Methods for Estimating the Hydraulic Properties of Unsaturated Soils, ed. M. Th. van Genuchten, F. J. Leij, and L. J. Lund, USDA ARS and University of Californina, Riverside, California.

Jury, W. A. and Horton, R. 2004. Soil Physics. 6th ed. John Wiley & Sons, Inc. Hobeken, New Jersey.

Klute, A. 1986. Methods of Soil Ananlysis, Part I. Physical and Mineralogical Methods, 2nd edition. Soil Science Society of America, Inc. Publisher, Madison, WI.

Munoz-Carpena, R., C. M. Regalado, J. Alvarez-Benedi, and F. Bartoli. 2002. Field evaluation of the new Philip-Dunne permeameter for measuring saturated hydraulic conductivity. Soil Science 167:9-24.

Philip, J. R. 1969. Theory of infiltration. Advanced Hydroscience. 5: 215-305.

Philip, J. R. 1993. Approximate Analysis of Falling-Head Lined Borehole Permeameter. Water Resources Research 29:3763-3768.

Rawls, W. J., Brakensiek, D. L., and Miller, N. 1983. Green-Ampt infiltration parameters from soils data. Journal of Hydraulic Engineering, ASCE, 109(1): 62–70.

Rousseeuw, P.J. 1990. Robust Estimation and Identifying Outliers in Handbook of Statistical Methods for Engineers and Scientists, edited by H.M. Wadsworth, New York: McGraw-Hill, pgs. 16.1–16.24.

Stephens, Michael A. 1986. Tests Based on EDF Statistics. Goodness of Fit Techniques. ed. Ralph B. D'Agostino and Michael A. Stephens. New York: Marcel-Dekker, pgs. 122-133.

Toothaker, Larry E. 1994. Multiple Comparison Procedures. Quantitative Applications in the Social Sciences. Newbury Park, California: Sage.

van Genuchten, M.Th. 1980. A closed-form equation for predicting the hydraulic conductivity for unsaturated soils. Soil Science Society of America Journal. 44:892-898.

Vogel, T., M. Cislerova, and J. W. Hopmans. 1991. Porous media with linearly variable hydraulic properties. Water Resources Research, 27(10): 2735-2741.

Winogradoff, Derek A. 2002. Bioretention Manual. Programs and Planning Division, Department of Environmental Resources, Prince George's County, Maryland.

Zhang, R. 1997. Determination of soil soptivity and hydraulic conductivity form the disk infiltrometer. Soil Science Society of America Journal. 61: 1024-1030.

Appendix A: Calculation Template for the MPD

A.1 Instructions for Use of the MPD Calculation Template

1. Open the Modified PD Calculation Template.xls file. If a Security Warning window appears select the Enable Marcos option.

2. Check to make sure the Solver Add-in is installed by clicking the *Check Solver Installation* button. If a message window appears that tells you "The solver add-in is not installed" click *OK* and continue with step 3. If the message window tells you "The solver add-in is installed" click *OK* and skip to step 4.

3. To install the Solver Add-in go the *Tools* menu, select *Add-Ins...* ,check the *Solver Add-in* box, and select *OK*. If Solver Add-in is not listed click *Browse* to locate it. If you see a message that tells you the Solver Add-in is not currently installed on your computer, click *Yes* to install it.

4. Enter data into C2:C6 as well as the time (in seconds) and height (in centimeters) below the appropriate column headings in cells G1 and H1.

5. Automatically fill all the rows in remaining columns by clicking the *Auto-fill Columns* button.

6. Calculate the distance to the wetting front at each time step by clicking the *Solve for R(t)* button.

7. Find values for mean hydraulic conductivity (K) and wetting front potential (C) by clicking the *Solve for K and C* button. Solver's solution for K and C will appear automatically in cells C11 and C12, respectively.

8. Repeat step 7 until the values for K and C remain constant.

9. Record values for K and C then click the *Clear Template* button. To perform another calculation repeat the procedure beginning at step 4.

A.2 Contents of the Excel® MPD Calculation Spreadsheet

The following material displays the contents of the Excel® spreadsheet used to calculate the mean hydraulic conductivity and wetting front potential as described above. Figure A.1 shows the cells in the Excel® MPD Calculation Template developed and Table A.1 contains the contents of the cells in the spreadsheet with formulas. Following the table is also the code for the macros written in Microsoft Visual Basic Application that are attached to the form buttons on the template (not shown in screenshot).

	A	B	C	D	E	F	G	H	I	J	O	P	Q	R
1	**Measured Variables**	**Notation**	**Value**	**Units**			t [sec]	h [cm]	q [cm/s]	R [cm]	dR/dt [cm/s]	ΔP [cm]	ΔP [cm]	Error^2
2	initial volumetric moisture	θ_i							n/a	2.76	n/a	n/a	n/a	0
3	final volumetric moisture	θ_f								6.02	n/a	n/a	n/a	0
4	length of device below surface	L_{max}		cm										
5	radius of device	r_1		cm										
6	phase one initial height	H_0		cm										
7														
8	**Computed Variables**	**Notation**	**Value**	**Units**										
9	change in volumetric moisture	$\Delta\theta$	0											
10	hemisperical source radius	r_0	0.00	cm										
11	wetting front potential	C	-100.00	cm										
12	mean hydraulic conductivity	K	1.00E-03	cm/s										
13	Sum of Error Squared		0											
14														
15														
16														
17														
18														
19														
20														
21														
22														
23														
24														
25														
26														
27														
28														

Figure A.1: Screenshot of the MPD Calculation Template.

Table A.1: Contents of the cells in the Excel(R) MPD Calculation Template that contain formulas.

Cell	Formula
C9	=C3-C2
C10	=C5/2
C13	=SUM(R:R)
I3	=(H3-H2)/(G3-G2)
J2	=IF(K2>=SQRT($C$4^2+$C$5^2),K2,"n/a")
J3	=IF(K3>=SQRT($C$4^2+$C$5^2),K3,"n/a")
L2	=($C$6-H2)*$C$5^2/$C$9
L3	=($C$6-H3)*$C$5^2/$C$9
M2	=(2*K2^3+3*K2^2*$C$4-$C$4^3-2*$C$10^3)/3
M3	=(2*K3^3+3*K3^2*$C$4-$C$4^3-2*$C$10^3)/3
N2	=L2-M2
N3	=L3-M3
O3	=IF(K2>=5*SQRT(2),(J3-J2)/(G3-G2),"n/a")
P2	=IF(O2<>"n/a",$C$11-(H2+I2*$C$4/$C$12+$C$4),"n/a")
P3	=IF(O3<>"n/a",$C$11-(H3+I3*$C$4/$C$12+$C$4),"n/a")
Q2	=IF(O2<>"n/a",(-$C$9*(J2^2+J2*$C$4)*O2/$C$12-2*$C$10^2)*(PI()^2/8)*LN((J2*($C$10+$C$4))/($C$10*(J2+$C$4)))/$C$4,"n/a")
Q3	=IF(O3<>"n/a",(-$C$9*(J3^2+J3*$C$4)*O3/$C$12-2*$C$10^2)*(PI()^2/8)*LN((J3*($C$10+$C$4))/($C$10*(J3+$C$4)))/$C$4,"n/a")
R2	=IF(O2<>"n/a",(P2-Q2)^2,"0")
R3	=IF(O2<>"n/a",(P2-Q2)^2,"0")

A.2.1 *Check Solver Installation* Macro

```
Sub Check_Solver_Installation()
Set a = AddIns("Solver Add-In")
If a.Installed = True Then
    MsgBox "The Solver add-in is installed"
Else
    MsgBox "The Solver add-in is not installed"
End If
End Sub
```

A.2.2 *Autofill Columns* Macro

```
Sub Autofill()
    x = 4
    'Loop until a blank row is found
    Do While Cells(x, 7).Value <> ""
        'This will fill in the remaining cells
        Cells(3, 9).Copy _
        Destination:=Cells(x, 9)
        Cells(3, 10).Copy _
        Destination:=Cells(x, 10)
        Cells(3, 11).Copy _
```

(Continued on next page)

```
      Destination:=Cells(x, 11)
      Cells(3, 12).Copy _
      Destination:=Cells(x, 12)
      Cells(3, 13).Copy _
      Destination:=Cells(x, 13)
      Cells(3, 14).Copy _
      Destination:=Cells(x, 14)
      Cells(3, 15).Copy _
      Destination:=Cells(x, 15)
      Cells(3, 16).Copy _
      Destination:=Cells(x, 16)
      Cells(3, 17).Copy _
      Destination:=Cells(x, 17)
      Cells(3, 18).Copy _
      Destination:=Cells(x, 18)
      'increase the value of x by 1 to act on the next row
      x = x + 1
   Loop
End Sub
```

A.2.3 *Solve for R(t)* Macro

```
Sub Solve_for_R()
x = 2
'repeat until blank
Do While Cells(x, 14).Value <> ""
SolverOk SetCell:=Cells(x, 14), _
   MaxMinVal:=3, _
   ValueOf:=0, _
   ByChange:=Cells(x, 11)
SolverSolve UserFinish:=True
x = x + 1
Loop
End Sub
```

A.2.4 *Solve for K and C* Macro

```
Sub Solve_for_K_and_C()
SolverOk SetCell:=Cells(13, 3), _
   MaxMinVal:=2, _
   ByChange:=Range(Cells(11, 3), Cells(12, 3))
   SolverSolve UserFinish:=True
End Sub
```

A.2.5 *Clear Template* Macro

```
Sub Clear_Template()
'clear columns
'start at row 4
```

```
x = 4
Do While Cells(x, 9) <> ""
   Cells(x, 9).ClearContents
   Cells(x, 10).ClearContents
   Cells(x, 11).ClearContents
   Cells(x, 12).ClearContents
   Cells(x, 13).ClearContents
   Cells(x, 14).ClearContents
   Cells(x, 15).ClearContents
   Cells(x, 16).ClearContents
   Cells(x, 17).ClearContents
   Cells(x, 18).ClearContents
   x = x + 1
Loop
'clear h vs t columns
'start at row 2
x = 2
Do While Cells(x, 7) <> ""
   Cells(x, 7).ClearContents
   Cells(x, 8).ClearContents
   x = x + 1
Loop
'clear cells C2:C6
Range("C2:C6").ClearContents
'set K and C to standard values
Range("C11").Formula = "-100"
Range("C12").Formula = ".001"
End Sub
```

Appendix B: Raw Data Included on Compact Disk

B.1 MPD Field Data

This folder includes all the MPD data collected at rain garden field sites during the summer of 2006. The data is grouped by field site and includes:

- a table of K_s results and site coordinates for the MPD tests,
- a figure of MPD test coordinate locations, and
- figures of head versus time curves for each MPD test performed.

Note that there are three different levels of detail collected for the head versus time curves. The most detailed curves (represented as solid lines) were produced from a MASSA ultrasonic sensor and other measures of head versus time were made manually with a piezometer tube and stopwatch (represented by a dot). In cases where only three data points existed in the head versus time curve (initial, midpoint, and final) an exponential decay function was fit to the data points to produce a "manufactured" head versus time curve (represented as a dashed line). See thesis by Asleson (2007) for evaluation of results.

B.2 MPD Lab Data

This folder includes all the MPD data collected in the laboratory and is grouped by barrel number. The file contains figures of the head versus time curve recorded by the MASSA ultrasonic sensor for MPD tests performed as well as the initial and final moisture content (see figure captions). Estimates of K_s and C were found as described in §3.3.3.

B.3 Mini Disk Lab Data

This folder contains files for each Minidisk test performed grouped by barrel number. Each file contains one test set which consists of five trials (see individual worksheet tabs). Estimates of hydraulic conductivity were obtained as described in §3.3.2 and the geometric mean of the five trials was used as the spatially averaged estimate of hydraulic conductivity.

B.4 Double Ring Lab Data

This folder contains files for each double ring test performed grouped by barrel number. See §3.3.1 for details on the reference falling head tests analysis.

B.5 Reference Falling Head Test Lab Data

This folder contains files for each reference falling head test performed grouped by barrel number. An additional overall summary file of the K_s results for each of the tests (with each barrel on separate worksheet tabs) is also included. See §3.3.4 for details on the reference falling head tests analysis.